prior to the 1:1 species), whose distinct features may be (i) that cimetidine is a tridentate ligand and hence the remaining one coordination site is open to incoming $O_2^-$, (ii) that cimetidine is a neutral ligand and hence the complexes bear positive net charges, ready to invite the attack of negative superoxide ion $O_2^-$, and (iii) that the Cu(I) $\rightleftharpoons$ Cu(II) conversion is nearly reversible without decomposition of the complexes. In Cu–SOD,[36] the Cu(II) in the active center is surrounded by four imidazole nitrogens and one $H_2O$ that is to be displaced by the incoming $O_2^-$. For further advantage Cu–SOD has Arg 141 (bearing a positive guanidinium cation, which helps to attract the negative $O_2^-$ to the $H_2O$ position.[37]

Recently, cimetidine has been reported to inhibit the oxidative metabolisms of steroid hormones,[38,39] drugs,[40–43] and other chemicals.[41] It was proposed that cimetidine directly binds at the sixth ligand position of cytochrome P-450.[44,45] Our present findings may invoke a new explanation that the active $O_2$ species formed on P-450 may be scavenged by the Cu–cimetidine complexes before they reach the substrates. We are planning to test this hypothesis. In this regard, it may be recalled that Cu(II) complexes of tyrosine, salicylates, etc. having SOD-like activities are also reported to inhibit drug metabolisms by microsomal cytochrome P-450.[46,47] In light of the recent report[48] that a Cu(II) complex of 3,5-diisopropylsalicylate exhibiting a strong SOD-like activity is promising as antiinflammatory and anticancer agents, the copper–cimetidine complexes are certainly worthy of thorough pharmacological investigations.

**Registry No.** $[CuL(H_2O)]ClO_4$, 102234-26-4.


(36) Tainer, J. A.; Getzoff, E. D.; Richardson, J. S.; Richardson, D. C. *Nature (London)* **1982**, *306*, 284.
(37) Getzoff, E. D.; Tainer, J. A.; Weiner, P. K.; Kollmann, P. A.; Richardson, J. S.; Richardson, D. C. *Nature (London)* **1983**, *306*, 287.
(38) Feely, J.; Robertson, D.; Island, D. P.; Wood, A. J. J. *N. Engl. J. Med.* **1982**, *306*, 1054.
(39) Morita, K.; Ono, T.; Shimakawa, H.; Wada, F. *Chem. Pharm. Bull.* **1984**, *32*, 4043.
(40) Knodell, R. G.; Holtzmann, J. L.; Crankshaw, D. L.; Stelle, N. M.; Stanley, L. N. *Gastroenterology* **1982**, *82*, 84.
(41) Pelkonen, O.; Puurunen, J. *Biochem. Pharmacol.* **1980**, *29*, 3075.
(42) Klotz, U.; Reimann, I. *N. Engl. J. Med.* **1980**, *302*, 1012.
(43) Desmond, P. V.; Patwardhan, R.; Parker, R.; Schenker, S.; Speeg, K. V. *Life Sci.* **1980**, *26*, 1261.
(44) Wilkinson, C. F.; Hetnarski, K.; Yellin, T. O. *Biochem. Pharmacol.* **1972**, *21*, 3187.
(45) Rendic, S.; Sunjic, V.; Toso, R.; Kajfez, F.; Ruf, H. *Xenobiotica* **1979**, *9*, 555.
(46) Richter, C.; Azzi, A.; Weser, U.; Wendel, A. *J. Biol. Chem.* **1977**, *252*, 5061.
(47) Werringloer, J.; Kawano, S.; Chacos, N.; Estabrook, R. W. *J. Biol. Chem.* **1979**, *254*, 11839.
(48) Sorenson, J. R. J. *Chem. Br.* **1984**, 1110.



Contribution from the Department of Chemistry,
The University of Houston—University Park, Houston, Texas 77004


# Electrochemistry of $[M(CO)_3Cp]_2$, $[M(CO)_3Cp]^+$, $[M(CO)_3Cp]^-$, and $M(CO)_3Cp$ Where M = Mo and W


K. M. Kadish,* D. A. Lacombe, and J. E. Anderson



*Received November 13, 1985*



The complete electrochemical mechanisms for the reduction and oxidation of $[Mo(CO)_3Cp]_2$ and $[W(CO)_3Cp]_2$, where Cp is cyclopentadienyl, and their associated monomeric cationic and anionic species were determined by the use of various electrochemical techniques. The dimers are both reduced and oxidized by an overall two-electron ECE mechanism, where the chemical reaction produces the monomeric 17-electron $M(CO)_3Cp$ radical (M = Mo, W). This radical is a key intermediate species in the electrochemical mechanism. It was demonstrated that $[Mo(CO)_3Cp]^+$ and $[M(CO)_3Cp]^-$ could be directly interconverted by a two-electron-transfer step. This latter reaction proceeds through the monomeric $M(CO)_3Cp$ radical species.


## Introduction

The heterometallic dimer (TPP)$InMo(CO)_3Cp$ and (TPP)-$InW(CO)_3Cp$, where TPP is the dianion of tetraphenylporphyrin,[1,2] may be oxidized or reduced by one or more electrons and, depending upon the potential, will generate as decomposition products either $[M(CO)_3Cp]_2$, $[M(CO)_3Cp]^+$, $[M(CO)_3Cp]^-$, or $M(CO)_3Cp$ where M = Mo or W.[2] In this regard, it is of some importance to understand the detailed electrochemistry of the molybdenum and tungsten complexes in the absence of a metalloporphyrin. This is the subject of the present communication.

The electrochemistry of Mo and W metal–metal-bonded complexes of the form $[M(CO)_3Cp]_2$ has been the subject of only several brief studies.[3–6] In nonaqueous media, the addition of two electrons to $[M(CO)_3Cp]_2$ generates the anionic $[M(CO)_3Cp]^-$ fragment, which is formed after rapid cleavage of the metal–metal bond. The abstraction of two electrons from $[M(CO)_3Cp]_2$ also results in rapid cleavage of the metal–metal bond, this time resulting in formation of $[M(CO)_3Cp]^+$. However, a complete electrochemical mechanism for these oxidations and reductions has never been reported. For example, the overall two-electron reduction of $[M(CO)_3Cp]_2$ can generate two $[M(CO)_3Cp]^-$ anions either by a single two-electron reduction, or by two one-electron reductions both of which are followed by cleavage of the metal–metal bond (an electrochemical EC or an EEC mechanism). Alternatively, the reduction may proceed first via the singly reduced $[M(CO)_3Cp]_2^-$ radical and then via the $M(CO)_3Cp$ fragment that is formed upon cleavage of the metal–metal bond in $[M(CO)_3Cp]_2^-$ (an electrochemical ECE mechanism).

The photolysis of $[M(CO)_3Cp]_2$ and $[W(CO)_3Cp]_2$ leads to homolytic cleavage of the metal–metal bond as shown in eq 1

$$[M(CO)_3Cp]_2 \xrightarrow{h\nu} 2M(CO)_3Cp \qquad (1)$$

where M = Mo[7,8] or W.[7,9] The $M(CO)_3Cp$ radical has also been postulated as an intermediate during electroreduction of the


(1) Cocolios, P.; Chang, D.; Vittori, P.; Guilard, R.; Moise, C.; Kadish, K. M. *J. Am. Chem. Soc.* **1984**, *106*, 5724.
(2) Kadish, K. M.; Guilard, R., manuscript in preparation.
(3) Madach, T.; Vahrenkamp, H. *Z. Naturforsch., B.: Anorg. Chem., Org. Chem.* **1979**, *34B*, 573.
(4) Dessy, R. E.; Stary, F. E.; King, R. B.; Waldrop, M. *J. Am. Chem. Soc.* **1966**, *88*, 471.
(5) Dessy, R. E.; Weissman, P. M.; Pohl, R. L. *J. Am. Chem. Soc.* **1966**, *88*, 5117.
(6) Denisovitch, L. I.; Gubin, S. P.; Chapovskii, Y. A.; Ustynok, N. A. *Bull. Acad. Sci. USSR, Div. Chem. Sci. (Engl. Transl.)* **1971**, *20*, 1851.
(7) Wrighton, M. S.; Ginley, D. S. *J. Am. Chem. Soc.* **1975**, *97*, 4246.
(8) Hughey, J. L.; Bock, C. R.; Meyer, T. J. *J. Am. Chem. Soc.* **1975**, *97*, 4440.
(9) Laine, R. M.; Ford, P. C. *Inorg. Chem.* **1977**, *16*, 388.



0020-1669/86/1325-2246$01.50/0

trimetallic compounds $M(CO)_3Cp–PtL_2–M(CO)_3Cp$ or $M(CO)_3Cp–Hg–M(CO)_3Cp$ in propylene carbonate.[10,11] This conclusion was based on peak potentials for oxidation and reduction of the W and Mo fragments as well as the presence of room-temperature ESR spectra that were assigned as due to $M(CO)_3Cp$. However, considering the rapid rate of redimerization of this species,[8] the observed ESR signal was probably due to a trapped species such as $M(CO)_3Cp(O_2)$. A similar species, $Mn(CO)_5O_2$, has been generated by reaction of $Mn(CO)_5$ with $O_2$.[16]

The $M(CO)_3Cp$ radical may be generated by electrooxidation of $[M(CO)_3Cp]^-$ or $[M(CO)_3Cp]_2$ or alternatively by electroreduction of $[M(CO)_3Cp]^+$ or $[M(CO)_3Cp]_2$. However, the direct observation of $M(CO)_3Cp$ has never been reported in the above electrochemical reactions. Thus, one object of this study is to present a systematic investigation of electrogenerated $Mo(CO)_3Cp$ and $W(CO)_3Cp$ radicals that are formed either by reduction or oxidation of the dimer, by oxidation of the monomeric anion, or by reduction of the monomeric cation. These results are then combined to present a comprehensive self-consistent oxidation–reduction mechanism of the investigated metal–metal-bonded complexes.

## Experimental Section

**Chemicals.** $[Mo(CO)_3Cp]_2$ and $[W(CO)_3Cp]_2$ were purchased from Alfa and used as received. The sodium salts of the monoanions were prepared by reduction of the corresponding dimers with a sodium amalgam in THF. Both the dimers and the anions were stored in a Vacuum Atmospheres drybox under an inert $N_2$ atmosphere. Tetrabutylammonium perchlorate (TBAP) was purchased from Fluka and was purified by recrystallization from a 20:80 mixture of hexane and ethyl acetate.

All solvents were freshly distilled before use and stored under nitrogen. Reagent grade methylene chloride ($CH_2Cl_2$) was distilled from $CaH_2$. Tetrahydrofuran (THF) was distilled under argon from a mixture of sodium and benzophenone. HPLC grade acetonitrile ($CH_3CN$) was refluxed for 1 h from $KMnO_4$, followed by distillation from $CaH_2$.

**Instrumentation.** All electrochemical measurements were performed with a BAS 100 electrochemical analyzer connected to a Houston Instruments HIPLOT DMP-40 plotter. Cyclic voltammetry and linear-sweep voltammetry were utilized with a three-electrode system. This consisted of a Pt-button working electrode (area = 0.7 $mm^2$), a Pt-wire counter electrode, and a silver-wire pseudoreference electrode. This electrode was separated from the bulk of the solution by a fritted glass bridge containing the supported electrolyte and solvent. Potentials of the $Fc^+/Fc$ couple were also measured with this electrode, and values of $E_{1/2}$ for each complex are then reported vs. a saturated calomel electrode (SCE) after correction with the ferrocene couple.

All voltammetric experiments werre carried out in a Vacuum Atmospheres drybox under a nitrogen atmosphere. Solutions contained 0.1 M tetrabutylammonium perchlorate (TBAP) as supporting electrolyte for all of the electrochemical experiments. All solvents were degassed with a stream of Linde prepurified argon for 10 min directly after distillation and before being introduced into the dry box. Experiments were run in the dark and in the light to test the photoactivity of the compound. The results of the experiments run in the dark were similar to those obtained in the light so that no special precautions were taken with respect to light.

## Results and Discussion

**Reactions of $[Mo(CO)_3Cp]_2$ and $[W(CO)_3Cp]_2$.** Cyclic voltammograms of $[Mo(CO)_3Cp]_2$ and $[W(CO)_3Cp]_2$ in THF, with 0.1 M TBAP as supporting electrolyte, are shown in Figure 1. For both complexes four sets of peaks are observed. This was true either for initial oxidation of the dimeric complexes (Figure 1a,c) or for initial reduction of the dimeric complexes (Figure 1b,d). The peaks in Figure 1 are labeled as I, II, III, and IV and correspond to the following general reactions where $M_2L_2$ represents $[Mo(CO)_3Cp]_2$ or $[W(CO)_3Cp]_2$ and ML represents one of the monomeric fragments.

$$M_2L_2 + 2e^- \xrightarrow{I} 2[ML]^- \quad (2)$$

$$2[ML]^- \xrightarrow{II} M_2L_2 + 2e^- \quad (3)$$

$$M_2L_2 \xrightarrow{III} 2[ML]^+ + 2e^- \quad (4)$$

$$2[ML]^+ + 2e^- \xrightarrow{IV} M_2L_2 \quad (5)$$

All four processes in Figure 1 are interrelated, and the four electrode reactions given by eq 2–5 give a reversible cyclical process. For example, the initial $[Mo(CO)_3Cp]_2$ is oxidized to form 2 equiv of $[Mo(CO)_3Cp]^+$ at $E_p$ = 0.97 V in THF (peak III), and this cationic species is reduced to regenerate $[Mo(CO)_3Cp]_2$ at $E_p$ = –0.52 V (peak IV). This dimer is then reduced by two electrons to give 2 equiv of $[Mo(CO)_3Cp]^-$ at $E_p$ = –1.20 V (peak I). Finally, the cyclical process is complete at $E_p$ = –0.17 V (peak II). At this potential $[Mo(CO)_3Cp]^-$ is oxidized to generate the original $[Mo(CO)_3Cp]_2$ dimer. A similar sequence of oxidation–reduction steps is observed for both series of complexes in $CH_2Cl_2$, THF, and $CH_3CN$, and the exact potentials for each of the four reactions are given in Table I.

Cyclic voltammograms of $[Mo(CO)_3Cp]_2$ and $[W(CO)_3Cp]_2$ were taken in $CH_2Cl_2$, THF, and $CH_3CN$, and analysis of each oxidation and reduction peak was carried out by using the criteria of Nicholson and Shain.[12,13] As seen in Figure 1 the shapes of the reduction peaks are broader than that predicted for a diffusion-controlled process, which would have $|E_p - E_{p/2}|$ values of 60 and 30 mV for $n$ = 1 and $n$ = 2, respectively. The experimentally observed $|E_p - E_{p/2}|$ for peak I depended upon the solvent system and varied between 110 and 121 mV for reduction of

**Table I.** Peak Potentials (V vs. SCE) for Oxidation and Reduction of the Dimeric, Anionic, and Cationic Species[a]

| metal syst | solvent | $M_2L_2$ oxidn (peak III) | $M_2L_2$ redn (peak I) | $[ML]^-$ oxidn (peak II) | $[ML]^+$ redn (peak IV) |
|---|---|---|---|---|---|
| Mo | $CH_2Cl_2$ | 1.00 | –1.21 | –0.09 | –0.42 |
| | THF | 0.97 | –1.20 | –0.17 | –0.52 |
| | $CH_3CN$ | 0.97 | –1.27 | –0.06 | –0.68 |
| W | $CH_2Cl_2$ | 1.00 | –1.31 | –0.06 | –0.53 |
| | THF | 1.04 | –1.19 | –0.07 | –0.52 |
| | $CH_3CN$ | 0.96 | –1.33 | –0.05 | –0.72 |

[a] All values were obtained at a scan rate of 0.2 V/s and were measured by using a Ag-wire pseudoreference electrode.

**Table II.** Values of $|E_p - E_{p/2}|$ (±5 mV) for Reduction and Oxidation of the Dimeric, Anionic, and Cationic Species

| metal syst | solvent | $M_2L_2$ oxidn (peak III) | $M_2L_2$ redn (peak I) | $[ML]^-$ oxidn (peak II) | $[ML]^+$ redn (peak IV) |
|---|---|---|---|---|---|
| Mo | $CH_2Cl_2$ | 60 | 110 | 55 | |
| | THF | 55 | 112 | 56 | 71 |
| | $CH_3CN$ | 62 | 115 | 65 | 89 |
| W | $CH_2Cl_2$ | 58 | 121 | 56 | 65 |
| | THF | 65 | 110 | 57 | 67 |
| | $CH_3CN$ | 66 | 111 | 56 | 70 |

**Table III.** Transfer Coefficients, $\alpha n$ (±0.05), for Reduction of $[Mo(CO)_3Cp]_2$ and $[W(CO)_3Cp]_2$ in Various Solvents

| compd | solvent | $\alpha n$ | compd | solvent | $\alpha n$ |
|---|---|---|---|---|---|
| $[Mo(CO)_3Cp]_2$ | $CH_2Cl_2$ | 0.54 | $[W(CO)_3Cp]_2$ | $CH_2Cl_2$ | 0.49 |
| | THF | 0.53 | | THF | 0.54 |
| | $CH_3CN$ | 0.51 | | $CH_3CN$ | 0.53 |
| | PhCN | 0.49 | | | |

(10) Giraudeau, A.; Lemoine, P.; Gross, M.; Braunstein, P. *J. Organomet. Chem.* **1980**, *202*, 455.
(11) Lemoine, P.; Giraudeau, A.; Gross, M.; Braunstein, P. *J. Chem. Soc., Chem. Commun.* **1980**, 77.
(12) Nicholson, R. S.; Shain, I. *Anal. Chem.* **1964**, *36*, 706.
(13) Nicholson, R. S.; Shain, I. *Anal. Chem.* **1965**, *37*, 178.
(14) Although an ESR spectrum of genuine $M(CO)_3Cp$ has never been reported, radicals of this type can be trapped with trace amounts of oxygen.[15,16] Under the proper conditions, an ESR signal is observed which is identical with that reported for $M(CO)_3(Cp)$,[10,11] believed to be a trapped species such as $M(CO)_3Cp(O_2)$.
(15) Waltz, W. L.; Hakelberg, O. H.; Dorfman, L. M.; Wojcicki, A. *J. Am. Chem. Soc.* **1978**, *202*, 455.
(16) Lindsell, W. E.; Preston, P. N. *J. Chem. Soc., Dalton Trans.* **1979**, 1105.

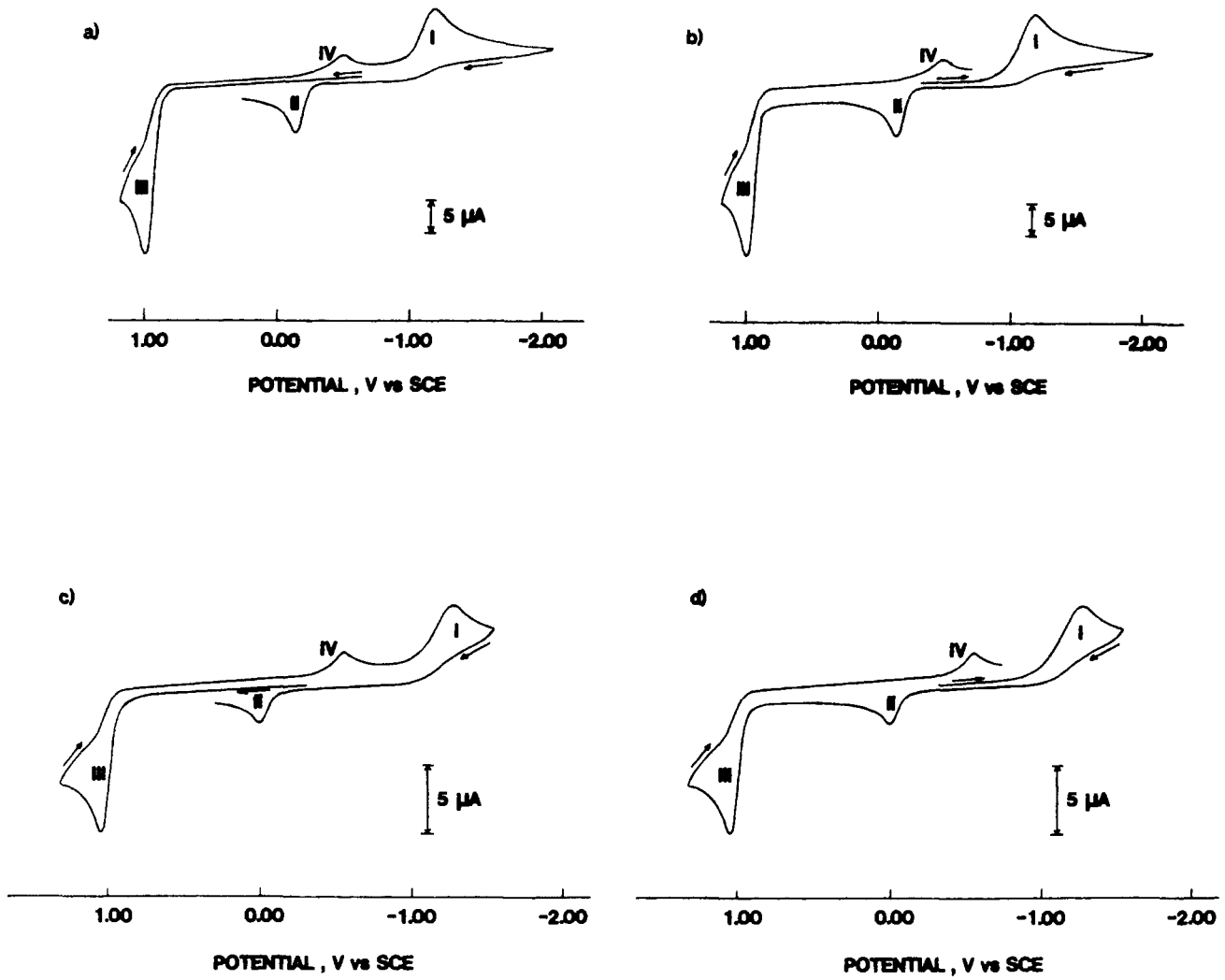


**Figure 1.** Cyclic voltammograms for (a) the initial oxidation of $[Mo(CO)_3Cp]_2$, (b) the initial reduction of $[Mo(CO)_3Cp]_2$, (c) the initial oxidation of $[W(CO)_3Cp]_2$, and (d) the initial reduction of $[W(CO)_3Cp]_2$ in THF with 0.1 M TBAP. Scan rate = 0.2 V/s.

$[Mo(CO)_3Cp]_2$ or $[W(CO)_3Cp]_2$. These peak separations are shown in Table II and can only be consistent with a rate-controlling (slow) electron transfer. Transfer coefficients, $\alpha n$, of 0.49–0.54 were calculated from this data. These values are listed in Table III.

The above voltammetric data suggest two plausible mechanisms for the reduction of $[Mo(CO)_3Cp]_2$ and $[W(CO)_3Cp]_2$. These are an electrochemical EEC mechanism and an electrochemical ECE mechanism. In the first mechanism, the complex would be reduced by two one-electron transfers to produce the doubly reduced dimer before cleavage of the metal–metal bond. In the second mechanism, the rate-determining addition of the first electron would be followed by cleavage of the metal–metal bond and then by a second one-electron reduction of the $M(CO)_3Cp$ radical to yield 2 equiv of the final anionic $[M(CO)_3Cp]^-$ product.

The formation of double reduced $[W(CO)_3Cp]_2^{2-}$ or $[Mo(CO)_3Cp]_2^{2-}$ has never been demonstrated, and an EEC mechanism seems highly unlikely given the apparent rapid cleavage of the metal–metal bond in $[M(CO)_3Cp]_2^-$. In addition, preliminary ESR results from monitoring the reaction intermediates indicate that the reduction of $[Mo(CO)_3Cp]_2$ and $[W(CO)_3Cp]_2$ proceeds via $Mo(CO)_3Cp$ or $W(CO)_3Cp$.[14] Thus, formation of these radicals is only consistent with the ECE mechanism shown in Scheme I.

**Scheme I**

$$[M(CO)_3Cp]_2 + e^- \rightleftarrows [M(CO)_3Cp]_2^- \quad (6)$$

$$[M(CO)_3Cp]_2^- \xrightarrow{\text{fast}} [M(CO)_3Cp]^- + M(CO)_3Cp \quad (7)$$

$$M(CO)_3Cp + e^- \rightleftarrows [M(CO)_3Cp]^- \quad (8)$$

The formation of $[M(CO)_3Cp]_2^-$ as the product of the first reduction (reaction 6) follows from the electrochemical data. This generated radical is not stable in solution, and rapid cleavage of the metal–metal bond will occur to give $[M(CO)_3Cp]^-$ and $M(CO)_3Cp$ as shown in eq 7. The generated $M(CO)_3Cp$ radical is electroreducible at the potential of $[M(CO)_3Cp]_2$ reduction, and the rapid addition of one electron to this radical (reaction 8) will lead to a second molecule of $[M(CO)_3Cp]^-$, thus giving the overall two-electron reduction shown in eq 2.

The other three electrode reactions shown in Figure 1 (peaks II–IV) are electrochemically irreversible in the sense that there are no coupled peaks on the return scan. However, the peak shapes are characterized by values of $|E_p - E_{p/2}|$ that are close to those expected for a reversible to quasi-reversible one-electron transfer. The exact values of $|E_p - E_{1/2}|$ are given in Table II. The experimentally observed 60 ± 5 mV peak separations for oxidation of $[Mo(CO)_3Cp]_2$ and $[W(CO)_3Cp]_2$ (peak III) are consistent with the ECE mechanism shown in Scheme II.

**Scheme II**

$$[M(CO)_3Cp]_2 \rightleftarrows [M(CO)_3Cp]_2^+ + e^- \quad (9)$$

$$[M(CO)_3Cp]_2^+ \xrightarrow{\text{fast}} [M(CO)_3Cp]^+ + M(CO)_3Cp \quad (10)$$

$$M(CO)_3Cp \rightleftarrows [M(CO)_3Cp]^+ + e^- \quad (11)$$

The first electrooxidation generates $[M(CO)_3Cp]_2^+$, which will cleave to give both $[M(CO)_3Cp]^+$ and $M(CO)_3Cp$. The latter radical is rapidly oxidized to give a second molecule of $[M(CO)_3Cp]^+$. This leads to the overall reaction shown in eq 4. The

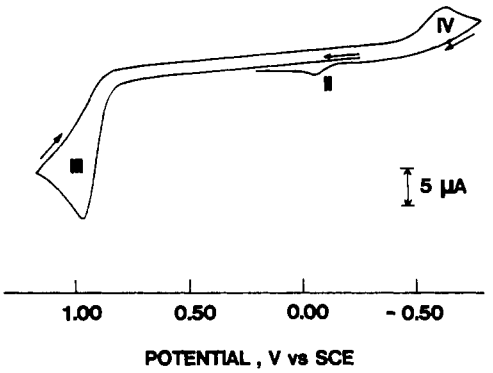


**Figure 2.** Cyclic voltammograms for the oxidation of $[Mo(CO)_3Cp]_2$ in $CH_3CN$ with 0.1 M TBAP at a Pt electrode. Scan rate = 0.4 V/s. Peak II illustrates the formation of $[Mo(CO)_3Cp]^-$ during the reduction of $[Mo(CO)_3Cp]^+$ at $E_p$ = –0.68 V (Peak IV).

generation of $[W(CO)_3Cp]^+$ or $[Mo(CO)_3Cp]^+$ as a product in the oxidation of the $[Mo(CO)_3Cp]_2$ and $[W(CO)_3Cp]_2$ dimers is indicated by the presence of peak IV, which only occurs after a global two-electron abstraction.

The potentials for peaks I–IV vary as a function of scan rate, and as the scan rate is increased, all of the peaks shift toward more difficult reactions (i.e., reduction peaks shift in a negative direction and oxidation peaks shift in a positive direction). These shifts in $E_p$ are due to the chemical reactions that follow each process, and the experimental magnitudes of the peak shifts are in general accordance with the presented mechanisms. A solvent effect on peak potentials is also observed for peaks I–IV (see Table I), and for the case of peak IV, the solvent effect is substantial. For example, at a scan rate of 0.2 V/s, $E_p$ = –0.42 V for the reduction of $[Mo(CO)_3Cp]^+$ in $CH_2Cl_2$ while in the more strongly bonding $CH_3CN$ the measured $E_p$ at this scan rate is –0.68 V. This negative shift of 0.26 V suggests a complexation of the electrogenerated cation with $CH_3CN$. This reaction is given by eq 12

$$[Mo(CO)_3Cp]^+ + CH_3CN \rightleftarrows [Mo(CO)_3Cp(CH_3CN)]^+ \quad (12)$$

for $Mo(CO)_3Cp$ and was first suggested by Pickett and Pletcher for the complexation of $[Mn(CO)_5]^+$ in $CH_3CN$.[17] A shift of 0.19 V is observed between $E_p$ for the reduction of $[W(CO)_3Cp]^+$ in $CH_2Cl_2$ (–0.53 V vs. SCE) and in $CH_3CN$ (–0.72 V vs. SCE), and this suggests that $[W(CO)_3Cp]^+$ is also coordinated by a solvent molecule. This solvation does not appear to influence the prevailing electrode mechanisms, and for the sake of clarity the cation is shown as uncomplexed in further mechanistic discussions.

**Electrode Reactions of $[M(CO)_3Cp]^+$ and $[M(CO)_3Cp]^-$.** Peak IV in Figure 1 illustrates the irreversible reduction of $[M(CO)_3Cp]^+$ to $[M(CO)_3Cp]_2$ while peak II illustrates the irreversible oxidation of $[M(CO)_3Cp]^-$ to $[M(CO)_3Cp]_2$. Both of these processes must pass through the $M(CO)_3Cp$ radical (reactions 13 and 14) prior to dimerization (reaction 15).

$$[M(CO)_3Cp]^+ + e^- \rightleftarrows M(CO)_3Cp \quad (13)$$

$$[M(CO)_3Cp]^- \rightleftarrows M(CO)_3Cp + e^- \quad (14)$$

$$M(CO)_3Cp \rightarrow {}^1/_2[M(CO)_3Cp]_2 \quad (15)$$

Dimerization rate constants for reaction 15 have been measured as $2 \times 10^9$ $M^{-1}$ $s^{-1}$ where M = Mo.[8] Thus, one might expect the dimer to be the ultimate product in both reactions 13 and 14. On the other hand, $M(CO)_3Cp$ can also be oxidized (reaction 11) or reduced (reaction 8), and the direct conversion of $[M(CO)_3Cp]^+$ to $[M(CO)_3Cp]^-$ as well as that of $[M(CO)_3Cp]^-$ to $[M(CO)_3Cp]^+$ is predicted from the potentials given in Table I. This overall two-electron transfer has been shown to occur[18] between $[Mn(CO)_5]^+$ and $[Mn(CO)_5]^-$ and also occurs between the two series

(17) Pickett, C. J.; Pletcher, D. *J. Chem. Soc., Dalton Trans.* **1975**, 879.
(18) Lacombe, D. A.; Anderson, J. E.; Kadish, K. M., *Inorg. Chem.* **1986**, *25*, 2074.

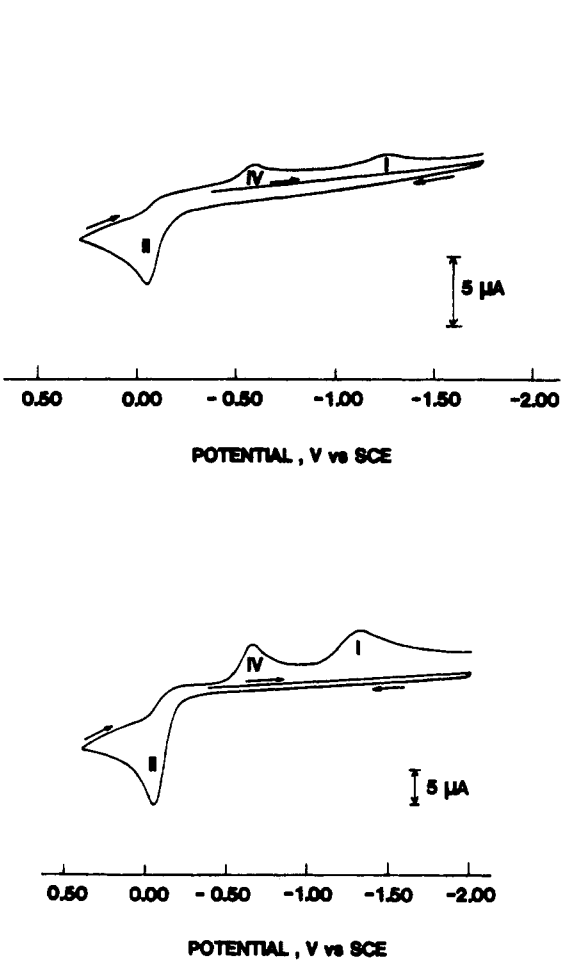


**Figure 3.** Cyclic voltammogram for the oxidation of (a) $[Mo(CO)_3Cp]^-$ and (b) $[W(CO)_3Cp]^-$ in $CH_3CN$ with 0.1 M TBAP at a Pt electrode. Scan rate = 0.2 V/s. Peak IV illustrates the formation of $[M(CO)_3Cp]^+$ during oxidation of $[M(CO)_3Cp]^-$ (Peak II).

**Scheme III**

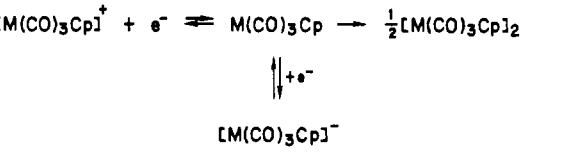


of compounds investigated in this study. This is illustrated by the cyclic voltammograms in Figures 2 and 3.

Figure 2 illustrates a cyclic voltammogram for the oxidation of $[Mo(CO)_3Cp]_2$ in $CH_3CN$ with 0.1 M TBAP. It also shows the electrochemistry of the generated oxidation products. As seen in this figure, $[Mo(CO)_3Cp]_2$ is oxidized to $[Mo(CO)_3Cp]^+$ (process III) during the first potential sweep, and on the return sweep, the generated $[Mo(CO)_3Cp]^+$ is reduced (process IV). However, in addition to the expected formation of $[Mo(CO)_3Cp]_2$ (reaction 5), the reduction of $[Mo(CO)_3Cp]^+$ also produces some $[Mo(CO)_3Cp]^-$. This is demonstrated by the presence of peak II, which occurs at $E_p$ = –0.06 V on the second positive sweep. This reaction corresponds to the oxidation of electrogenerated $[Mo(CO)_3Cp]^-$. No currents are observed on the first positive sweep, thus indicating that $[Mo(CO)_3Cp]^-$ is generated as a product in the reduction at –0.68 V. Thus, the relevant mechanism for the two-electron reduction of $[M(CO)_3Cp]^+$ and the generation of $[M(CO)_3Cp]^-$ is given by Scheme III. In this scheme, the oxidation of $[M(CO)_3Cp]^+$ leads first to $M(CO)_3Cp$, which can either dimerize or abstract a second electron to give $[M(CO)_3Cp]^-$. The data in Figures 1 and 2 suggest that both reactions occur.

Evidence for formation of $[M(CO)_3Cp]^+$ from $[M(CO)_3Cp]^-$ comes from the voltammograms shown in Figure 3. This figure illustrates cyclic voltammograms for the oxidation of [Mo-

**Scheme IV**

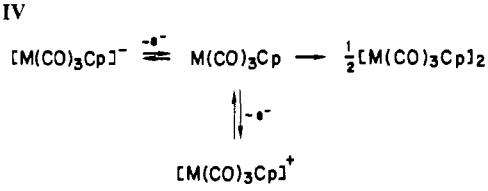


$(CO)_3\dot{C}p]^-$ and $[W(CO)_3Cp]^-$ in $CH_3CN$ with 0.1 M TBAP. In both cases, oxidation of the anion (process II) leads to $[M(CO)_3Cp]^+$. The formation of the cation is demonstrated by the appearance of peak IV on the second negative potential sweep. This peak does not appear on the first negative sweep and thus suggests the reactions given in Scheme IV. The peak potential for the $[W(CO)_3Cp]^-/W(CO)_3Cp$ couple (reaction 14) is at −0.05 V in $CH_3CN$ (Figure 3b) as compared to a peak potential of −0.72 V for the $[W(CO)_3Cp]^+/W(CO)_3Cp$ couple (reaction 13). Thus, at −0.05 V one would expect $[W(CO)_3Cp]^-$ to be oxidized directly to $[W(CO)_3Cp]^+$, and this is what is observed in Figure 3b. Likewise, thermodynamics also favor the formation of $[Mo(CO)_3Cp]^+$ from $[Mo(CO)_3Cp]^-$, and this is illustrated by the presence of peak IV in Figure 3a. In this regard, it should be noted that $[M(CO)_3Cp]_2$ is the product of both $[M(CO)_3Cp]^-$ oxidation and $[M(CO)_3Cp]^+$ reduction. Thus, the presence of both peaks IV and I in Figure 3 follows from the fact that the dimer is inevitably the only species at the electrode surface when potentials sufficiently negative to cause its reduction are reached.

A key point in Schemes I–IV is the presence of the $M(CO)_3Cp$ radical. This species is formed by oxidation or reduction of $[M(CO)_3Cp]_2$ as well as by oxidation of $[M(CO)_3Cp]^-$ or reduction of $[M(CO)_3Cp]^+$. A combined, overall oxidation–reduction mechanism for the interconversion of $[M(CO)_3Cp]_2$, $[M(CO)_3Cp]^-$, and $[M(CO)_3Cp]^+$ is presented in Figure 4. The importance of the $M(CO)_3Cp$ radical is clear. In addition to the major reaction pathways of $M(CO)_3Cp$, the reaction of $O_2$ with

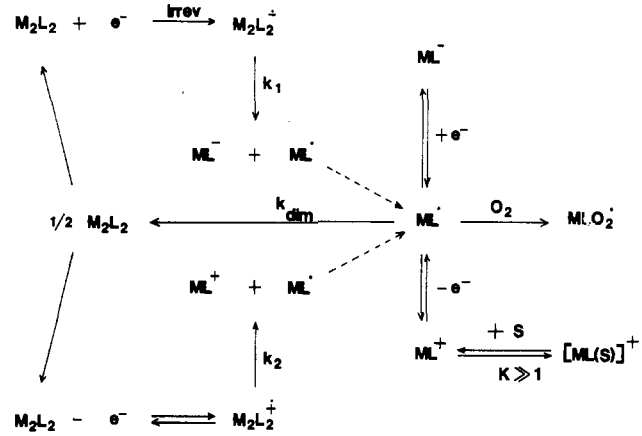


**Figure 4.** Overall mechanism for the electrochemical interconversion of $[M(CO)_3Cp]_2$, $[M(CO)_3Cp]^+$, $[M(CO)_3Cp]^-$, and $M(CO)_3Cp$ where M = Mo and W. These species are represented by $M_2L_2$, $[ML]^+$, $[ML]^-$, and ML.

the species is indicated. This reaction will particularly allow for indirect observation of $M(CO)_3Cp$ by ESR spectroscopy.[14] This scheme is similar to that reported for the oxidation and reduction of $Mn_2(CO)_{10}$,[18] and this similarity in the oxidation or reduction of three metal–metal-bonded dimers suggests that this type of mechanism may be general to systems of this type.

**Acknowledgment.** The support of the National Science Foundation (Grant CHE-8215507) is gratefully acknowledged. We also acknowledge helpful conversations with Dr. Paul Lemoine, who read a preliminary draft of the manuscript.

**Registry No.** $[Mo(CO)_3Cp]_2$, 12091-64-4; $[W(CO)_3Cp]_2$, 12091-65-5; $[Mo(CO)_3Cp]^-$, 12126-18-0; $[W(CO)_3Cp]^-$, 12126-18-0; $[Mo(CO)_3Cp]^+$, 12126-17-9; $[W(CO)_3Cp]^+$, 102262-08-8; $Mo(CO)_3Cp$, 12079-69-5; $W(CO)_3Cp$, 12079-77-5; Mo, 7439-98-7.

---

Contribution from the Department of Chemistry, The University of Houston—University Park, Houston, Texas 77004, and Laboratoire de Synthèse et d'Electrosynthèse Organométallique associé au CNRS (UA33), Faculté des Sciences "Gabriel", University of Dijon, 21100 Dijon, France

# Electrochemical Studies of Dimeric Niobium(V) Porphyrins. Reactions of $[(OEP)Nb]_2O_3$ and $[(TpTP)Nb]_2O_3$ in Nonaqueous Media

J. E. Anderson,[1a] Y. H. Liu,[1a] R. Guilard,[1b] J.-M. Barbe,[1b] and K. M. Kadish*[1a]

*Received November 18, 1985*

The electrochemistry and spectroelectrochemistry of $[(P)Nb]_2O_3$, where P is the dianion of either octaethylporphyrin (OEP) or tetra-*p*-tolylporphyrin (TpTP), is reported in five different nonaqueous solvents. These Nb(V) dimers may undergo up to three reductions and three oxidations depending upon the solvent/supporting electrolyte system and temperature. ESR measurements on the bulk-electrolyzed solutions are combined with electrochemical and spectroelectrochemical data to present an overall electrooxidation/reduction mechanism for the two dimeric complexes.

## Introduction

Monomeric Nb(V) porphyrins of the type (P)Nb(O)(X) and $(P)Nb(X)_3$ have been characterized, where P is the dianion of a given porphyrin macrocycle and X is a halogen.[2-6] The crystal structure of (P)Nb(O)(F)[7] and $(P)Nb(O)(O_2CCH_3)$[2] show that the Nb(V) atom is above the plane of the porphyrin ring and that the other axial ligands assume a cis geometry with respect to the porphyrin ring. The acetate group in $(OEP)Nb(O)(O_2CCH_3)$ is bidentate in the solid state. The same unusual geometry is also adopted by Nb(V) in $[(P)Nb]_2O_3$ where P = OEP, TPP, and TpTP.[2,8,9] These dimeric complexes have three oxygen atoms,

(1) (a) The University of Houston. (b) University of Dijon.
(2) Lecomte, C.; Protas, J.; Guilard, R.; Fliniaux, B.; Fournari, P. *J. Chem. Soc., Dalton Trans.* **1979**, 1306.
(3) Lecomte, C.; Protas, J.; Guilard, R.; Fliniaux, B.; Fournari, P. *J. Chem. Soc., Chem. Commun.* **1976**, 435.
(4) Buchler, J. W.; Rohbock, K. *Inorg. Nucl. Chem. Lett.* **1972**, *8*, 1073.
(5) Gouterman, M.; Hanson, L. K.; Khalil, G.-E.; Buchler, J. W.; Rohbock, K.; Dolphin, D. *J. Am. Chem. Soc.* **1975**, *97*, 3142.
(6) Green, M. L. H.; Moreau, J. J. E. *Inorg. Chim. Acta* **1978**, *31*, L461.
(7) Lecomte, C.; Protas, J.; Richard, P.; Barbe, J.-M.; Guilard, R. *J. Chem. Soc., Dalton Trans.* **1982**, 247.
(8) Johnson, J. F.; Scheidt, W. R. *J. Am. Chem. Soc.* **1977**, *99*, 294.

0020-1669/86/1325-2250$01.50/0 